

Progressive Failure Analysis and Failure Map into Plain Weave Glass Fibre Reinforced Polymer Bolted Joint

Khudhayer J. Jadee *

Technical Engineering College-Baghdad, Middle Technical University, Baghdad, Iraq
*Corresponding author: khudhayer1970@yahoo.com

Received August 19, 2015; Revised August 25, 2015; Accepted August 28, 2015

Abstract The performance of the glass fibre reinforced polymer (GFRP) composite bolted joint has been investigated using experimental and finite element methods. The glass fibre reinforcement was plain weave fabric of 800g/m² weight. The investigation has been carried out on a double-lap composite bolted joint with many geometric parameters. Progressive failure analysis has been conducted using Hashin failure criteria to determine the failure load, failure mode and bearing strength. Failure map has been also defined with respect to the geometric parameters.

Keywords: bolted joint, progressive failure analysis, GFRP, failure map

Cite This Article: Khudhayer J. Jadee, "Progressive Failure Analysis and Failure Map into Plain Weave Glass Fibre Reinforced Polymer Bolted Joint." *American Journal of Materials Science and Engineering*, vol. 3, no. 2 (2015): 21-28. doi: 10.12691/ajmse-3-2-1.

1. Introduction

There are many methods to assemble between the composite parts, such as bonded joint, mechanical fastening joint, or combination of them. Bolted joint is one type of mechanical fastening method, which is preferred due to low cost, free surface treatment [1,2], and the simplicity in repair and maintenance [3].

The finite element method (FEM) is normally used to determine the stress distribution in fibre-reinforced composite structures with bolted joints. Many finite element programs are currently available, such as NASTRAN, COSMOL, ABAQUS, and ANSYS.

In general, the laminate is considered to have failed when a lamina fails, which is known as the first ply failure (FPF) and leads to a reduction in the stiffness of the joint [4]. The laminate continues to sustain more loads until the

final failure takes place, which is called the last ply failure (LPF) [5].

After the stress distribution around the bolted joint has been determined, failure criteria are used to determine if the laminate has failed at a certain point. To predict the failure load, the bearing strength of the composite bolted joint, and failure propagation, failure criteria should be used in conjunction with progressive failure analysis. The strength properties of the failed elements should be replaced by suitable new strength properties according to the degradation rule and the failure mode until the final failure.

In general there are three ways for composite bolted joints to fail, net-tension, shear-out, and bearing modes. Combinations of these failure modes (mixed mode) may be possible. Figure 1 illustrates these modes schematically [6,7,8,9].

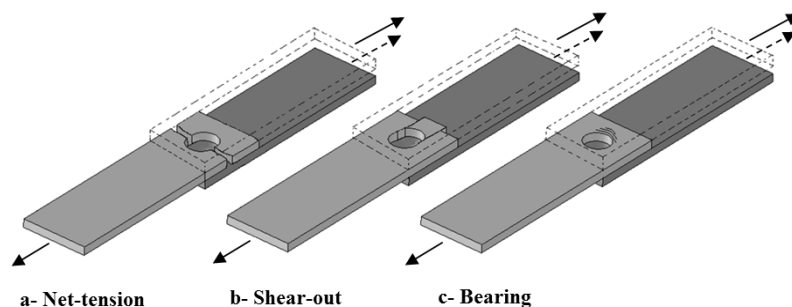


Figure 1. Common failure modes in bolted composite plates

There are three main categories of failure criteria used to predict the failure of the laminated composite; independent, interactive and separate mode criteria. Separate mode Hashin failure criterion was selected in this

work because it consists of five in-plane failure modes to predict the failure of laminated composite plate [10].

Failure analysis usually applies when predicting the strength and failure mode of lamina. Many failure criteria

can be used in conjunction with progressive failure analysis by adopting the finite element method. Failure criteria are classified as an independent, interactive, and a separate mode criterion. Progressive failure analysis involves three steps, which are stress analysis, failure analysis, and the material property degradation rule [11].

Independent criteria (or limit criteria) such as maximum stress and maximum strain criteria predict the failure load and failure mode by evaluating the stresses in the lamina and comparing it separately with the corresponding strengths and neglecting the interaction among these stresses [12]. However, it is the easiest to apply.

Interactive criteria such as Tsai-Wu, Hoffman and Tsai-Hill criteria predict the failure load by using a quadratic or polynomial equation involving all the stress components. Failure is assumed when the equation is satisfied. First ply failure can be predicted using this criterion; however, the main disadvantage of these criteria is the lack of failure mode [13].

Separate mode criteria such as Hashin criterion separates the fibre failure criterion from the matrix failure criterion and may depend on one or more stress components. 2-D Hashin failure theory involves five in-plane failure modes to predict the failure of the laminates [10]. These failure modes are as follows:

- Matrix tensile failure
- Matrix compression failure
- Fibre-matrix shearing failure
- Fibre tensile failure
- Fibre compression failure

The objective of this study is to investigate the plain weave glass fibre reinforced polymer bolted joint using progressive failure analysis method and to obtain the failure map of the composite bolted joint using both experimental and finite element methods.

2. Experimental Work

Vacuum bagging technique has been used to fabricate the glass fibre reinforced polymer (GFRP) laminates. The laminates consist of eight plies of glass fibre plain weave fabric with a weight of 800g/m² impregnated with epoxy. Epoxy resin (CP 216Z2 PART A) and hardener (CP 216Z2 PART B) were mixed in a ratio of 2:1 by weight as a matrix material. All the plies principal direction aligned in the same direction [0]^o. A continual vacuum of -1 bar was applied to the bagging package inside an oven and the laminate was firstly heated at a rate of 1.7°C/minute until the oven temperature reaches 80°C, then holding at 80°C for two hours followed by cooling to room temperature at a rate of 1.7°C/minute before removed from the oven. The obtained laminate was of 5.2 mm thickness.

A jig saw with tungsten carbide blade has been then used to cut the laminates to the required size, followed by a final finishing to reduce the edge delamination. Then, undersize holes were drilled followed by reaming to achieve the final hole diameter (8mm). A dummy composite plate was attached under the laminates during the drilling in order to minimize the hole edge damage. All composite coupons were designed with a width to bolt diameter (W/D) and edge distance to bolt diameter (E/D) varied as (2,3,4,5) and (1,2,3,4,5), respectively. While the thickness (t), the bolt-hole diameter (D), and the free

length (L) were kept constant at a value of; 5.2, 8, and 140mm, respectively. The coupon's geometry of the laminates is illustrated in Figure 2.

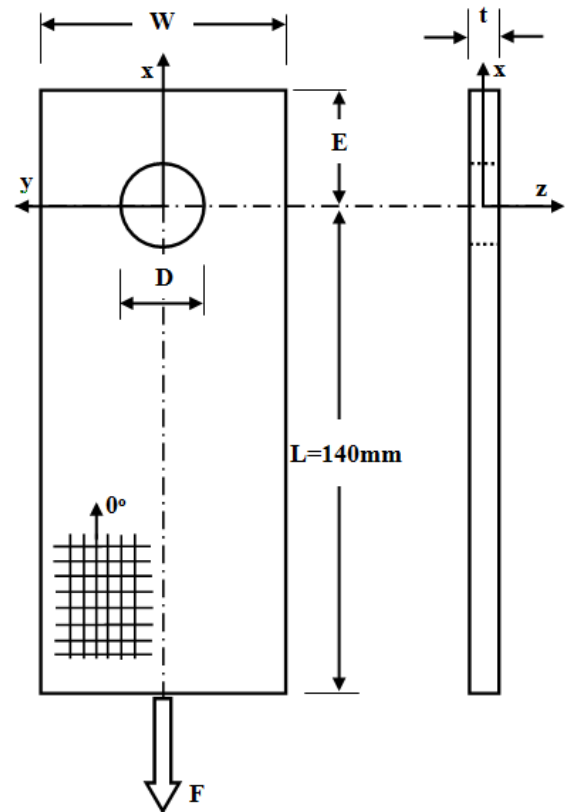


Figure 2. Coupon geometry

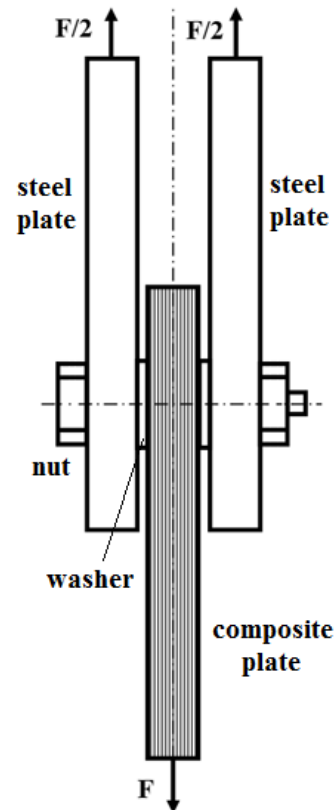


Figure 3. Composite bolted joint

Bearing test has been carried out according to the ASTM standard D 5961/D 5961M-10 procedures A [14] using INSTRON 3367 universal testing machine of 30 kN

loading capacity in tensile loading at a rate of 0.5 mm/min. The composite specimen was connected to two steel plates with the aid of finger tightened bolt, which represents the lowest bolt torque [15]. Two steel washers were inserted between the composite specimen and the steel plates. For all tests, the principal fibres direction of the composite specimen aligned with the load direction. The joint configuration illustrated in Figure 3.

3. Finite Element Method

The performance of composite bolted joint with single-bolt, double-lap configuration, subjected to tensile loading has been analysed using the finite element method (FEM) based on ANSYS code.

SOLID185 element has been used to simulate the laminate. This element is a 3-D layered structural solid element defined by eight nodes with three degrees of freedom at each node, translations in the nodal x, y, and z directions. This element available in two options; homogeneous structural solid (KEYOPT K3=0) and layered structural solid (KEYOPT K3=1) which usually used to simulate the layered thick shells or solids. Higher concentration of the elements around the hole has been set to provide better accuracy.

The mechanical properties of the 800g/m² plain weave GFRP lamina have been determined experimentally, and listed in Table 1. In general, balanced plain weave structure has two fibre directions (weft and warp), assuming one direction with the applied load and the other perpendicular to the applied load.

Table 1. Mechanical properties of 800g/m² plain weave GFRP laminate

Parameters	Symbol (Units)	Values	Standard test method
Longitudinal modulus	E_1 (MPa)	17129	ASTM D3039
Transverse modulus	E_2 (Mpa)	17129	ASTM D3039
Shear Modulus	G_{12} (Mpa)	3693	ASTM D3518
Poisson's ratio	ν_{12} (-)	0.24	ASTM D3039
Longitudinal tension strength	X_t (Mpa)	222.14	ASTM D3039
Longitudinal compression strength	X_c (Mpa)	96.7	ASTM D3410
Transverse tension strength	Y_t (Mpa)	222.14	ASTM D3039
Transverse compression strength	Y_c (Mpa)	96.7	ASTM D3410
Laminate shear strength	S (Mpa)	65.27	T-specimen [16,17,18,19]

Only half of the model has been used for analysis due to the symmetry with respect to xz plane as shown in

Figure 4. Therefore, the displacement of the nodes in the symmetry axis was constrained in the y direction.

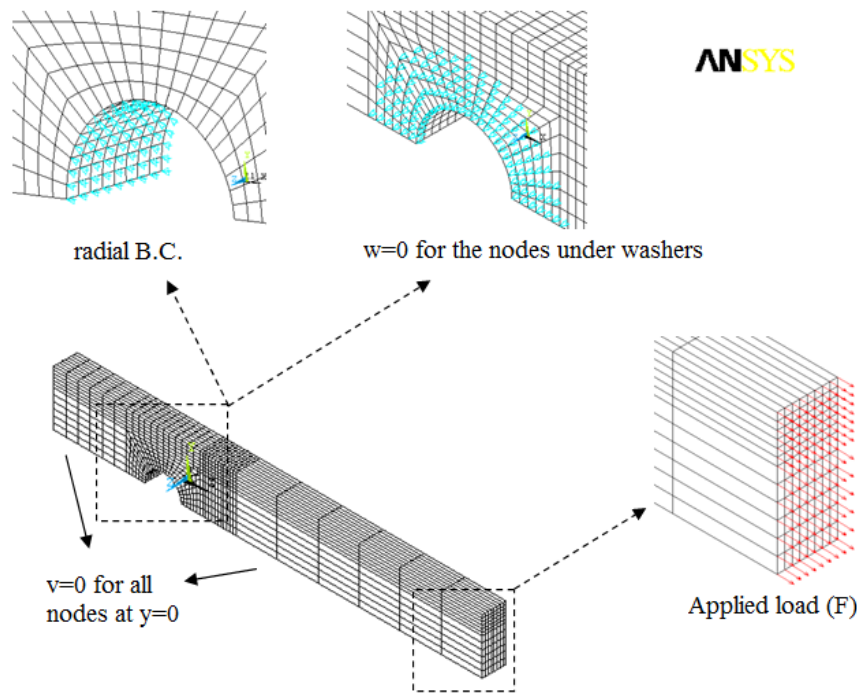


Figure 4 Finite element model

Uniform distributed tensile load was applied to the nodes at the far end of the composite. In addition, radial boundary condition was applied for all nodes in the whole area in contact with bolt, these nodes are constrained in the radial direction and free in the circumferential direction [2,16,20,21,22]. To simulate the finger tight torque, all the nodes on the surface under the washers were constrained in the z-direction.

3.1. 2-D Progressive failure analysis model

Progressive failure analysis involves three stages, including the stress analyses to assess the in-plane stresses in the material axis; longitudinal (σ_1), transverse (σ_2) and shear (τ_{12}). The second stage is the failure analysis using Hashin failure criteria, followed by the last stage, which is the material properties degradation rule to the failed elements.

ANSYS APDL code has been written for progressive failure analysis to determine the failure load, failure mode, and the bearing strength of the laminated bolted joint. The flowchart of the progressive failure analysis code is highlighted in the algorithm shown in Figure 5. Firstly, stress analysis of the laminate was conducted, followed by the failure analysis to check for the failed elements. If failed elements were detected, then a suitable material degradation rule would apply (the third stage) according to the failure mode. Otherwise, the applied load would be increased according to the input of load increment. A small load increment would achieve high precision results; hence, the step load increment (ΔF) was set at 1.025 of the previous load. These processes continued until the final failure.

To distinguish the damaged elements according to the failure mode, six different colours for the element were applied.

After the stress analysis and strength prediction of the laminate, a failure analysis has been performed accordingly, followed by the material property degradation rule. As detailed in Table 2.

In general, five strength properties are required to define the in-plane failure of the ply under multi-axial stress system (X_t , X_c , Y_t , Y_c , and S). In addition, three in-plane stresses (σ_1 , σ_2 and τ_{12}) are required for the failure analysis.

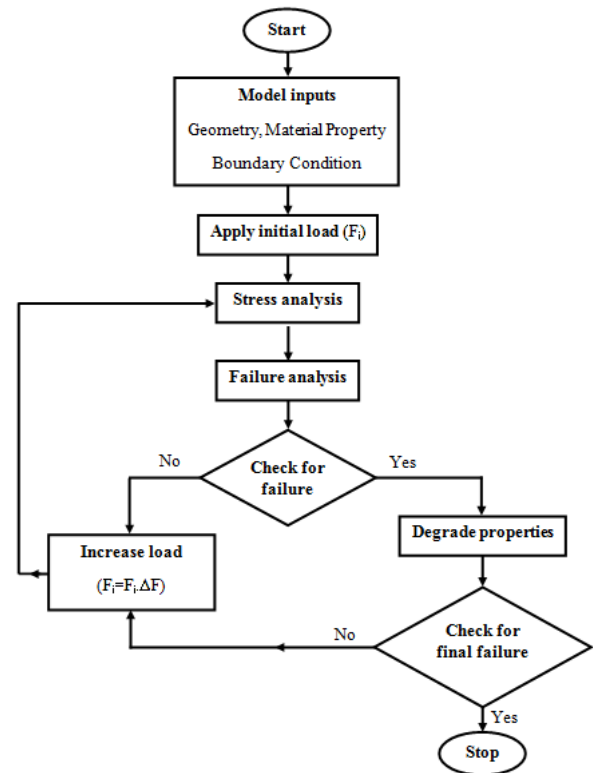


Figure 5. Flow chart for the progressive failure model

Table 2 Hashin failure criteria

Failure mode	Failure criteria	Element colour	Material properties degradation rule
Matrix tensile failure ($\sigma_2 > 0$)	$\left(\frac{\sigma_2}{Y_t}\right)^2 + \left(\frac{\tau_{12}}{S}\right)^2 \geq 1$		Y_t, E_2, ν_{12} reduced to zero
Matrix compression failure ($\sigma_2 < 0$)	$\left(\frac{\sigma_2}{Y_c}\right)^2 + \left(\frac{\tau_{12}}{S}\right)^2 \geq 1$		Y_c, E_2, ν_{12} reduced to zero
Fibre-matrix shearing failure ($\sigma_1 < 0$)	$\left(\frac{\sigma_1}{X_c}\right)^2 + \left(\frac{\tau_{12}}{S}\right)^2 \geq 1$		S, G_{12} reduced to zero
Fibre tensile failure ($\sigma_1 > 0$)	$\left(\frac{\sigma_1}{X_t}\right)^2 + \left(\frac{\tau_{12}}{S}\right)^2 \geq 1$		$X_t, X_c, Y_t, Y_c, S, E_1, E_2, G_{12}, \nu_{12}$ reduced to zero
Fibre compression (or bearing) failure ($\sigma_1 < 0$)	$\left(\frac{\sigma_1}{X_c}\right)^2 \geq 1$		$X_t, X_c, Y_t, Y_c, S, E_1, E_2, G_{12}, \nu_{12}$ reduced to zero

3.2. Verification of Finite Element Models

Previous literature work was selected for the verification of the progressive failure analysis model. The work is related to the study of the progressive failure analysis of open-hole quasi-isotropic carbon/epoxy composite laminates with stacking sequence [45/0/-45/90]_s subjected to remote tension [23]. The geometry and boundary conditions of the laminate used in that work are presented in Figure 6.

The authors used different failure theories, including the micro-mechanics of failure, maximum stress, Tsai-Wu, Hashin, and Puck theories with ABAQUS user subroutine to analyse the open-hole laminate. Moreover, mesh

dependency was investigated using four different meshes with 168, 400, 600, and 864 elements. The stress at the first load drop (first fibre rupture) was considered as the ultimate strength. The ultimate strength and damage patterns were obtained by that work.

On the other hand, the present work has been completed with the ANSYS program, using SOLID185 element. An APDL subroutine of progressive failure analysis was used to compare the failure pattern and ultimate strength with the results of Liu et al. The verifications also involved the mesh dependency. For this purpose four different meshes with 200, 400, 600, and 800 elements were compared with the previous work.

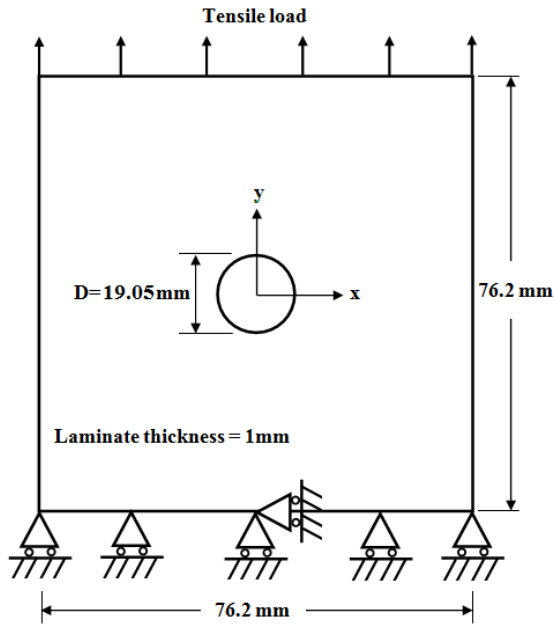


Figure 6. Geometric and boundary conditions of the open-hole laminate [23]

4. Results and Discussion

4.1. Progressive Failure Model Verification

The comparison of failure propagation of Hashin's failure theory is shown in Figure 7. It is clear that the failure pattern is almost the same for all plies for fibre and matrix failures. In Liu's et al. work the experimental failure load at the first fibre rupture was 30259 N, while the failure load obtained from the progressive failure analysis using ABAQUS was 27477.7N which give (9% variation from the experimental load).

In the present model the failure load is 28170N, which gives a 6.9% variation compared to the experimental failure load and a 2.4% variation from the Liu et al. model.

Mesh dependency analysis was also carried out. Four different mesh densities were selected in the previous model for this purpose (168, 400, 600, and 864 elements), while another four mesh densities (200, 400, 600, and 800 elements) were selected for the present model. The comparison between the two models is illustrated in Figure 8. The present model achieved stable mesh dependency between 600 and 800 elements.

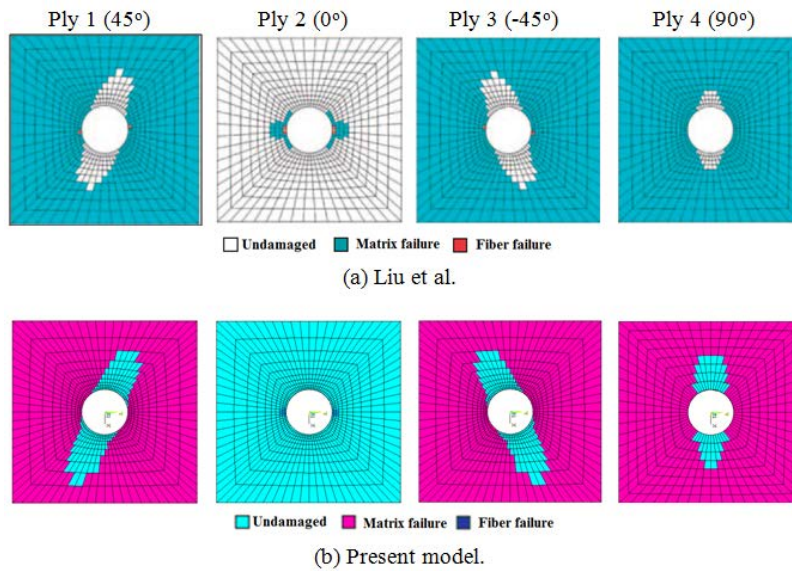


Figure 7. Damage pattern comparison between Liu et al. and present model

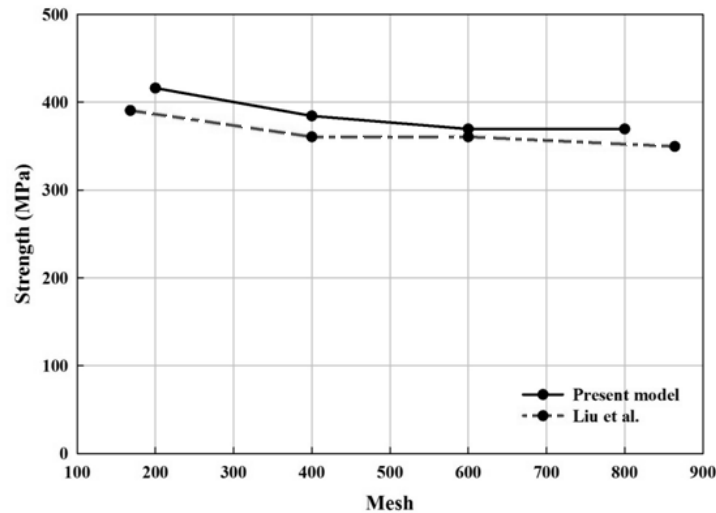


Figure 8. Mesh dependency

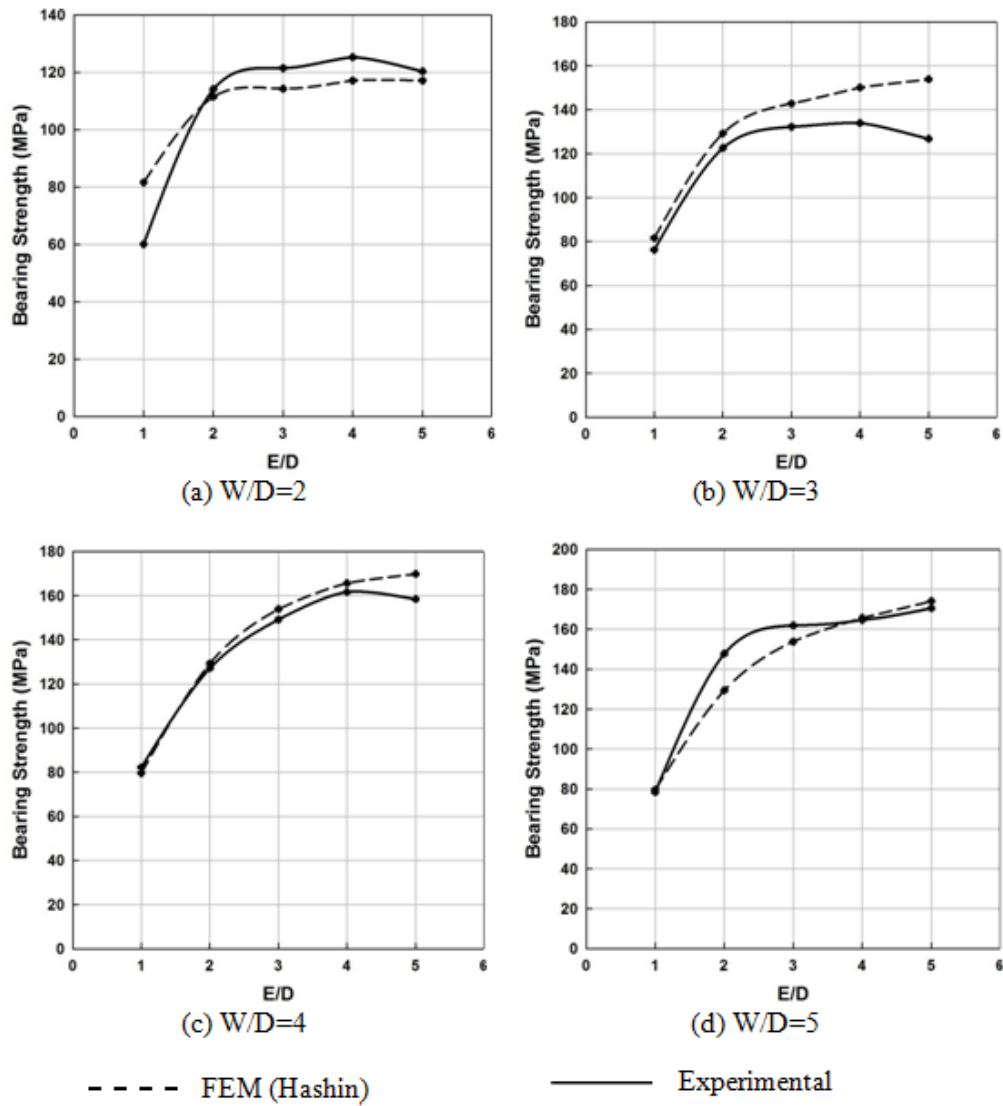


Figure 9. Variation of bearing strength

4.2. Numerical and Experimental Strength Evaluation

The bearing strength of the experimental results was compared with those of the finite element analysis results for all E/D and W/D values. Hashin failure criterion was used for the failure analysis to determine the failure load and bearing strength. These results are shown in Figure 9. The predictive finite element results show an acceptable correlation with the experimental results.

4.3. Failure Analysis

Progressive failure analysis was performed to assess the failure mode of the laminated composite bolted joints. The Hashin failure criterion was used for this purpose, whereby the load was gradually applied and all elements were checked for failure. If the element fails, the degradation rule was applied to that element according to the failure type, and then the load continued until final failure.

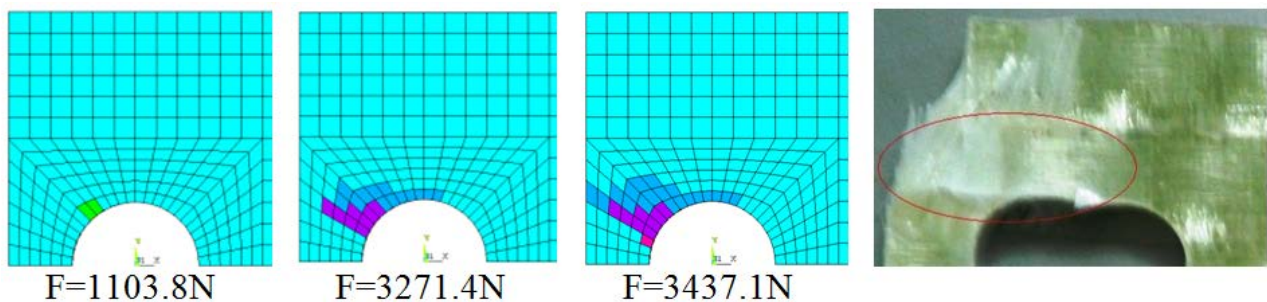


Figure 10. Failure propagation of laminate with W/D=4 and E/D=1; shear-out failure

Figure 10 shows the propagation of failure for the laminate with W/D=4 and E/D=1. The failure propagates

gradually as the applied load is increased until the failure propagates along the shear-out plane to the laminate edge;

this failure mode is identified as shear-out failure. Shear-out failure occurs in laminates with a small edge distance.

Net-tension failure mode is illustrated in Figure 11, whereby the failure propagates along the net-tension plane of laminate with $W/D=2$ and $E/D=3$ until it reaches the

width edge. This mode of failure is the net-tension mode and occurs in narrow width laminates.

For a wide laminate with a long edge distance, the failure propagation is illustrated in Figure 12. The damage is concentrated in fibre compression in the bearing area opposite to the bolt providing the bearing failure mode.

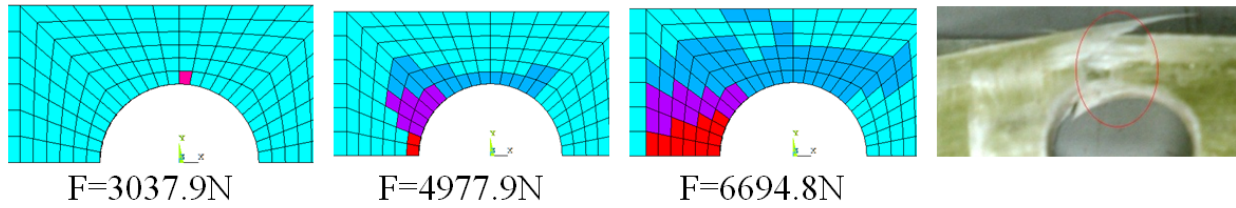


Figure 11. Failure propagation of laminate with $W/D=2$ and $E/D=3$; net-tension failure

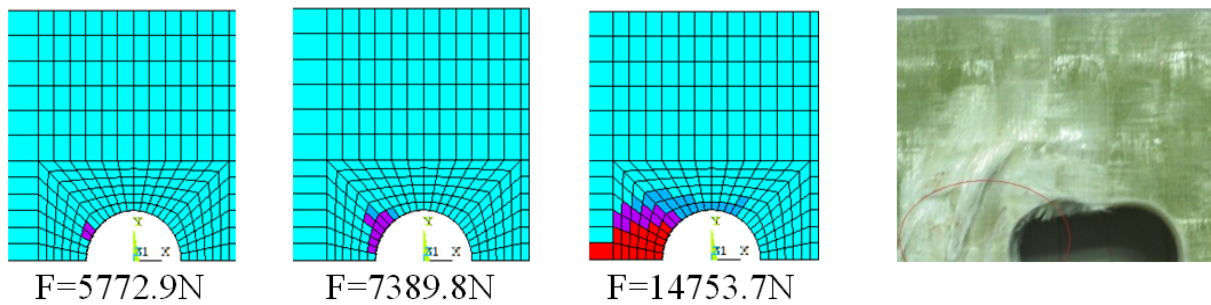


Figure 12. Failure propagation of laminate with $W/D=5$ and $E/D=5$; bearing failure

The above shown results confirm that providing a sufficient large end distance (E) and width (W), tension and shear out failures could be suppressed and achieve full bearing strength potential [8].

A comprehensive F.E.M and experimental failure map for all ranges of laminate geometry is shown in Table 3. A strong correlation between the experimental and F.E.M. was achieved.

Apparently, for a wide laminate ($W/D \geq 3$) with long edge distance ($E/D \geq 3$), the failure is bearing mode, while in narrow laminate ($W/D=2$), the failure mode is net-tension, except for small edge distance ($E/D=1$) which is shear-out failure.

In laminates with short edge distance ($E/D=1$), the dominant failure mode is shear-out for all W/D values. It is clear that when the W/D and E/D ratios increase beyond a certain value (≥ 3), the failure mode changes from shear-out or net-tension to bearing failure, which is the desired failure mode. This finding agrees with previous literature works [18,24].

5. Conclusions

Experimental bearing test and progressive failure analysis on a double-lap, single-bolt joints in the GFRP composite structure have been carried out to determine the failure load, failure mode and bearing strength. Hashin failure criteria has been adopted for the progressive failure analysis as it involves five in-plane failure modes to predict the failure of the laminate. Progressive failure analysis and mesh dependency showed acceptable results. The predictive finite element results for the bearing strength showed acceptable correlation with the experimental results. In addition, the failure map predicted by the progressive failure analysis has been compared with the experimental failure mode for a wide range of geometric parameters and showed a strong correlation.

It was found that the laminates with wide and long edge distance ($W/D \geq 3$ and $E/D \geq 3$) showed a signs for the bearing failure. Whilst, the net-tension failure was predominant for the narrow laminates ($W/D=2$), except for the small edge distance ($E/D=2$). All the short edge laminates ($E/D=1$), the failure mode was the shear-out failure mode.

References

- [1] Choi JH, Ban CS, Kweon JH, Failure load prediction of a mechanically fastened composite joint subjected to a clamping force, *Journal of composite materials*, 42(14). 1415-1428. July 2008.
- [2] Ryu CO, Choi JH, Kweon JH, Failure load prediction of composite joints using linear analysis, *Journal of composite materials*, 41.865-878. April 2007.
- [3] Goswami S, A finite element investigation on progressive failure analysis of composite bolted joints under thermal environment,

Table 3. Failure mode of laminates with all W/D and E/D

W/D		E/D				
		1	2	3	4	5
2	Experimental	S	B-S	N	N	B-N
	F.E.M.	S	B-S	B-N	B-N	B-N
3	Experimental	S	B-S	B	B	B
	F.E.M.	S	B-S	B	B	B
4	Experimental	S	B-S	B	B	B
	F.E.M.	S	B-S	B	B	B
5	Experimental	B-S	B-S	B	B	B
	F.E.M.	S	B-S	B	B	B

S=shear-out, N= net-tension, B= bearing, B-S= bearing shear-out failure mode.

- Journal of reinforced plastics and composites*, 24. 161-171. January 2005.
- [4] Dano ML, Gendron G, Picard A, Stress and failure analysis of mechanically fastened joints in composite laminates, *Composite structures*, 50(3). 287-296. November 2000.
- [5] Ekh J, *Multi-fastener single-lap joints in composite structures*, in Department of aeronautical and vehicle engineering., Royal institute of technology: Stockholm, Sweden. 2006
- [6] Chang FK, Scott RA, Springer GS, Strength of mechanically fastened composite joints, *Journal of composite materials*, 16(6). 470-494. November 1982.
- [7] Sen F, et al, Experimental failure analysis of mechanically fastened joints with clearance in composite laminates under preload, *Materials and design*, 29(6). 1159-1169. January 2008.
- [8] Yılmaz T, Sýnmazçelik T, Investigation of load bearing performances of pin connected carbon/polyphenylene sulphide composites under static loading conditions, *Materials and design*, 28(2). 520-527. January 2007.
- [9] Aktas A, Dirikolu M, An experimental and numerical investigation of strength characteristics of carbon-epoxy pinned-joint plates, *Composites science and technology*, 64(10-11). 1605-1611. August 2004.
- [10] Lessard LB, Shokrieh MM, Two-dimensional modeling of composite pinned-joint failure, *Journal of composite materials*, 29(5). 671-697. March 1995.
- [11] Zhang J, Rowland J, Damage modeling of carbon-fiber reinforced polymer composite pin-joints at extreme temperatures, *Composite structures*, 94(8). 2314-2325. July 2012.
- [12] Hart-Smith LJ, The role of biaxial stresses in discriminating between meaningful and illusory composite failure theories, *Composite structures*, 25(1-4). 3-20. October 1992.
- [13] Dato MH, *Mechanics of fibrous composites*, Elsevier applied science, 1991.
- [14] ASTM D 5961M-10, Standard test method for bearing response of polymer matrix composite laminates, *American society for testing of materials*, 2010.
- [15] McCarthy M, McCarthy C, Finite element analysis of effects of clearance on single shear composite bolted joints, *Plastics, rubber and composites*, 32(2). 65-70. February 2003.
- [16] Okutan B, The effects of geometric parameters on the failure strength for pin-loaded multi-directional fiber-glass reinforced epoxy laminate, *Composites part B: Engineering*, 33(8). 567-578. November 2002.
- [17] Aktas A, Karakuzu R, Failure analysis of two-dimensional carbon-epoxy composite plate pinned joint, *Mechanics of composite materials and structures*, 6(4). 347-361. October 1999.
- [18] Okutan B, Aslan Z, Karakuzu R, A study of the effects of various geometric parameters on the failure strength of pin-loaded woven-glass-fiber reinforced epoxy laminate, *Composites science and technology*, 61(10). 1491-1497. August 2001.
- [19] İçten BM, Okutan B, Karakuzu R, Failure strength of woven glass fiber-epoxy composites pinned joints, *Journal of composite materials*, 37(15). 1337-1350. August 2003.
- [20] Karakuzu R, Çalışkan CR, Aktaş M, İçten BM, Failure behavior of laminated composite plates with two serial pin-loaded holes, *Composite structures*, 82(2). 225-234. January 2008.
- [21] Karakuzu R, Taylak N, İçten BM, Aktaş M, Effects of geometric parameters on failure behavior in laminated composite plates with two parallel pin-loaded holes, *Composite structures*, 85(1). 1-9. September 2008.
- [22] Karakuzu R, Gülem T, İçten BM, Failure analysis of woven laminated glass-vinylester composites with pin-loaded hole, *Composite structures*, 72(1). 27-32. January 2006.
- [23] Liu G, Tay TE, and Tan VB, Failure progression and mesh sensitivity analyses by the plate element-failure method, *Journal of composite materials*, 44(20). 2363-2379. September 2010
- [24] Asi, O, Effect of different woven linear densities on the bearing strength behaviour of glass fiber reinforced epoxy composites pinned joints, *Composite structures*, 90(1). 43-52. September 2009.